Research article

JHEP|Reports

C/EBPβ–VCAM1 axis in Kupffer cells promotes hepatic inflammation in MASLD

Authors

Shuang-Zhe Lin, Yang Xie, Yu-Qing Cheng, …, Mingxi Liu, Yuan-Wen Chen, Jian-Gao Fan

Correspondence

chenywhdgi@fudan.edu.cn (Y.-W. Chen), fanjiangao@xinhuamed.com.cn (J.-G. Fan).

Graphical abstract

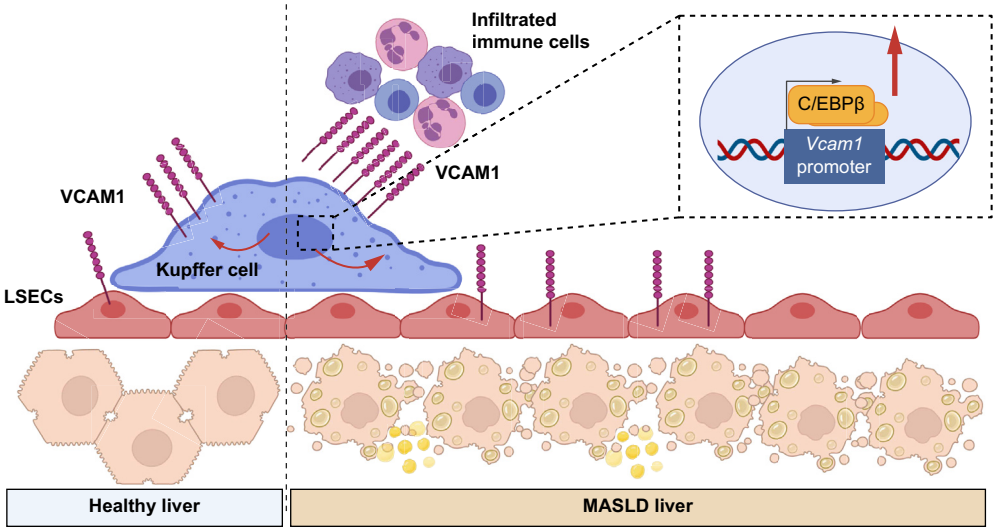

Highlights:

- The MASLD liver microenvironment induces increased C/EBPβ levels in Kupffer cells.
- C/EBPβ selectively promoted MASLD-induced genes in Kupffer cells.
- C/EBPβ can directly induce VCAM1 expression in Kupffer cells.
- Kupffer cell-expressed VCAM1 in MASLD promotes hepatic inflammatory cell infiltration.

Impact and implications:

Metabolic dysfunction-associated steatotic liver disease (MASLD) is the most common chronic liver disease worldwide, but its pathogenesis remains elusive. In this study, we investigated the critical role of CCAAT/enhancer binding protein β (C/EBPβ) in Kupffer cells and its implications in MASLD pathogenesis. We found that an increased C/EBPβ level in Kupffer cells promotes hepatic inflammation in MASLD by upregulating VCAM1 expression. Our findings provide valuable insights into the molecular mechanisms driving MASLD and propose a potential novel therapeutic target to mitigate hepatic inflammation in MASLD.

https://doi.org/10.1016/j.jhepr.2025.101418

Research article

JHEP|Reports

C/EBPβ–VCAM1 axis in Kupffer cells promotes hepatic inflammation in MASLD

Shuang-Zhe Lin[1,†], Yang Xie[1,†], Yu-Qing Cheng[1], Rui Xue[1], Yin-Shi Su[2], Mingxi Liu[3], Yuan-Wen Chen[2,4,*], Jian-Gao Fan[1,5,*]

JHEP Reports **2025**. vol. 7 | 1–14

Background & Aims: Kupffer cells (KCs) can promote hepatic inflammation in metabolic dysfunction-associated steatotic liver disease (MASLD), but the underlying molecular mechanisms are not fully understood. C/EBPβ in macrophages can mediate metabolic and immune dysregulations. Therefore, we aimed to explore its role in KCs in MASLD pathogenesis.

Methods: A 12-week high-fat and high-cholesterol diet (HFHCD) model was used in wild-type or KC-specific *Cebpb* heterozygous knockout mice (n = 10 per group), followed by liver evaluation using histopathology, flow cytometry, and RNA-seq. RNA-seq of liver tissue (n = 3 per group) and C/EBPβ CUT&Tag-seq of sorted KCs were comprehensively analyzed to elucidate the transcriptional regulatory network. Flow cytometry and immunofluorescence were used to detect the expression or distribution of key proteins.

Results: HFHCD induced prominent immune cell infiltration and a concomitant increase in C/EBPβ in KCs. KC-specific *Cebpb* heterozygous knockout significantly reduced HFHCD-induced lobular inflammation (p <0.05) and inflammation-related gene expression (p <0.05) in the liver. Multi-omics analysis revealed increased C/EBPβ activity in KCs in MASLD, leading to a selective promotive effect on MASLD-induced genes. Further integrated analysis identified *Vcam1* as a key direct downstream gene of C/EBPβ in KCs in MASLD, which involves C/EBPβ-mediated activation of the *Vcam1* promoter. VCAM1 was predominantly expressed in KCs in the hepatic tissue of MASLD mice and patients. KC-expressed VCAM1 was significantly increased in MASLD compared with healthy controls (p <0.01), and it promoted immune cell infiltration into the liver.

Conclusions: Increased C/EBPβ in KCs promotes pathogenic transcriptional activation, leading to increased VCAM1 expression and inflammatory cell infiltration in MASLD. Inhibition of C/EBPβ in KCs might be a potential therapeutic strategy against hepatic inflammation in MASLD.

Introduction

Metabolic dysfunction-associated steatotic liver disease (MASLD) refers to a disease spectrum that includes metabolic dysfunction-associated steatotic liver (MASL) and metabolic dysfunction-associated steatohepatitis (MASH). It is the most common cause of chronic liver disease worldwide, jeopardizing nearly one-fourth of the global population.[1] The severe form MASH can increase the risk of developing liver fibrosis and end-stage liver diseases.[2] Hepatic inflammation is an important pathological process in MASLD development. It can exacerbate liver tissue damage and promote fibrosis progression.[3,4] In addition, liver inflammation *per se* is associated with increased all-cause mortality in patients with MASLD.[5] Therefore, there is an urgent need for a deeper understanding of the pathophysiology of hepatic inflammation in MASLD.

The liver is enriched in various types of immune cells, including macrophages.[6] Hepatic macrophages are highly heterogeneous and can be primarily divided into two major subsets according to differences in ontogeny and cellular phenotype: Kupffer cells (KCs) and monocyte-derived macrophages (MoMFs). Compared with the highly heterogeneous MoMFs originating from peripheral blood monocytes, KCs are tissue-resident macrophages located in the hepatic sinusoids and are characterized by relative homogeneity and liver-related specialized functions.[7–9] In the healthy liver, most KCs are derived from fetal monocytes and keep self-renewal after birth (*i.e.* embryonic KCs [EmKCs]). In MASLD, EmKCs are partially replaced by KCs derived from peripheral monocytes (*i.e.* monocyte-derived KCs [MoKCs]). More importantly, KCs were found to undergo significant changes in transcriptome and cellular functions.[10–12] These changes in KCs may facilitate the onset and progression of hepatic inflammation in MASLD, but pertinent details remain elusive.

* Corresponding authors. Addresses: Department of Gastroenterology, Huadong Hospital, Fudan University, Shanghai 200040, China. Tel.: +86-21-62483180 (Y-W. Chen); Department of Gastroenterology, Xin Hua Hospital affiliated to Shanghai Jiao Tong University School of Medicine, Shanghai 200092, China. Tel.: +86-21-25078999 (J-G. Fan).
E-mail addresses: chenywhdgi@fudan.edu.cn (Y.-W. Chen), fanjiangao@xinhuamed.com.cn (J.-G. Fan).
† These authors contributed equally to this work.
https://doi.org/10.1016/j.jhepr.2025.101418

The cellular development and functions of macrophages are highly complicated and variable and require fine-tuning from the transcriptional regulatory network. The *cis–trans* interactions between transcription factors (TFs) and genomic cis-regulatory elements (CREs) play a pivotal role in this network.[13] In KCs, LXR is a well-characterized lineage-determining factor indispensable for KC-specific functions, whereas ATF3 and p300 have been identified as stimulus-regulated factors in the context of MASLD, contributing to further transcription reprogramming and disease-associated cellular phenotypes.[14,15] Our previous study demonstrated that a TF called CCAAT/enhancer binding protein β (C/EBPβ) can promote pro-inflammatory chemokine C–C motif chemokine 5 expression in hepatocytes, thus inducing MASLD progression.[16] C/EBPβ has long been implicated in both metabolic and immune dysregulations.[17,18] In the liver, C/EBPβ is highly expressed in both hepatocytes and macrophages.[19] However, the specific role of C/EBPβ in MASLD-related transcriptional regulation of KCs remains elusive. Therefore, we hypothesize that C/EBPβ can selectively modulate transcriptional dysregulation in KCs and contribute to hepatic inflammation progression in MASLD.

Materials and methods

Animal experiments

Cebpb$^{fl/fl}$ mice (Cat. No. T013481) and *Clec4f*-iCre-2A-tdTomato mice (Cat. No. NM-KI-200069) were purchased from GemPharmatech Co. Ltd. (Nanjing, China) and Shanghai Model Organisms Center (Shanghai, China), respectively. Rosa26-ACTB-mTdTomato-mEGFP mice (Cat. No. 007676) were purchased from Jackson Laboratory and were bred with *Clec4f*-iCre-2A-tdTomato mice to generate Rosa26-ACTB-mTdTomato-mEGFP; *Clec4f*-iCre mice. Male wild-type mice (aged 6–8 weeks) were purchased from Jihui Laboratory Animal Co. Ltd. (Shanghai, China). The MASLD model was constructed using a high-fat and high-cholesterol diet (HFHCD).[20] Briefly, 12 week-old mice were fed with HFHCD (88% standard diet, 10% lard, and 2% cholesterol by weight) for 12 weeks. Mice in the control group were fed a normal diet (ND). All mice were in a C57BL/6J background and housed in a 12-h light/dark cycle in a temperature-controlled room under specific pathogen-free conditions, with free access to food and water. Mice were euthanized at the indicated time points by exsanguination after CO_2 anesthesia to collect liver and serum samples. All animal studies were conducted at Shanghai Rat & Mouse Biotech Co. and were approved by the Institutional Animal Care and Use Committee of Shanghai Rat & Mouse Biotech Co. (SHRM-IACUC-060) in adherence to NIH guidelines for the use of experimental animals.

Human samples

Formalin-fixed paraffin-embedded liver samples were collected from patients clinically diagnosed with MASH (n = 3) and healthy controls (n = 2) at the Department of Gastroenterology, Xinhua Hospital of Shanghai Jiao Tong University School of Medicine, from September 2020 to October 2023. None of the patients had hepatitis virus infection, excessive alcohol consumption, drug abuse, Wilson's disease, autoimmune-related disorders, or cancer. The research protocol was approved by the Research and Ethics Committee of Xinhua Hospital, and all research was conducted in accordance with both the Declarations of Helsinki and Istanbul. Before the initiation of the study, written informed consent was acquired from all participants (Approval No. XHEC–NSFC–2021-209). sc/snRNA-seq data of the human liver were obtained from a previous study[21] (GSE192742).

Statistical analysis

Data are presented as bar charts with mean ± SEM or violin plots. Differences were considered statistically significant at $p < 0.05$. Please refer to the figure legends for the detailed methods of hypothesis testing.

Results

KCs in MASH participate in hepatic inflammation and highly express C/EBPβ

We first established a murine MASLD model in wild-type C57BL/6J mice using HFHCD.[20] After 12 weeks of feeding, key histological features of MASLD were recapitulated, including significant hepatic steatosis, ballooning, intralobular inflammation, and an increase in the NAS score (Fig. 1A and B). In terms of leukocyte distribution, CD45$^+$ leukocytes were sparsely distributed in normal livers, and most leukocytes in the hepatic lobules were CLEC4F$^+$ KCs. In contrast, there were aggregates of immune cells (*i.e.* inflammatory foci) in hepatic lobules of HFHCD-fed mice in addition to sparsely distributed KCs (Fig. 1C). Notably, these aggregates were composed of both infiltrated non-KC leukocytes (CD45$^+$ CLEC4F$^-$) and KCs (Fig. 1C), indicating the participation of KCs in inflammatory foci formation. In addition, metabolic indices, including body weight, liver index, and epididymal fat weight, were also significantly increased (Fig. 1D). We further made a rudimentary identification of EmKC (mostly CLEC4F$^+$VSIG4$^+$) and MoKC (mostly CLEC4F$^+$VSIG4$^-$). We found that CLEC4F$^+$VSIG4$^-$ cells were exclusively present in the livers of HFHCD-fed mice, but not in those of ND-fed mice, as previously reported. More importantly, both CLEC4F$^+$VSIG4$^+$ and CLEC4F$^+$VSIG4$^-$ cells were involved in these inflammatory foci (Fig. S1A), indicating co-participation of EmKCs and MoKCs in inflammatory foci formation. We then quantified the numeric changes in KCs (F4/80^{hi} CD11b^{int}) and non-KC myeloid cells (F4/80^{int} CD11b^{hi}, mainly composed of infiltrated MoMFs and neutrophils) (Fig. S1B). We found significantly increased proportions of non-KC myeloid cells among total leukocytes in HFHCD-fed mice and decreased KC/non-KC myeloid cell ratio (Fig. 1E). In addition, intracellular staining of C/EBPβ revealed that HFHCD induced a significant increase in C/EBPβ protein level in KCs (Fig. 1F).

C/EBPβ in KCs promotes hepatic inflammation in MASH

To target C/EBPβ knockdown in KCs, we used the Cre-loxP system to construct KC-specific *Cebpb* monoallelic knockout (*Clec4f*-iCre;*Cebpb*$^{fl/+}$) mice and used littermate (*Clec4f*-iCre;*Cebpb*$^{+/+}$) mice as controls. The expression specificity of Cre recombinase was validated using cre-reporter mice (Fig. S2A), and intracellular staining of C/EBPβ verified that KC-

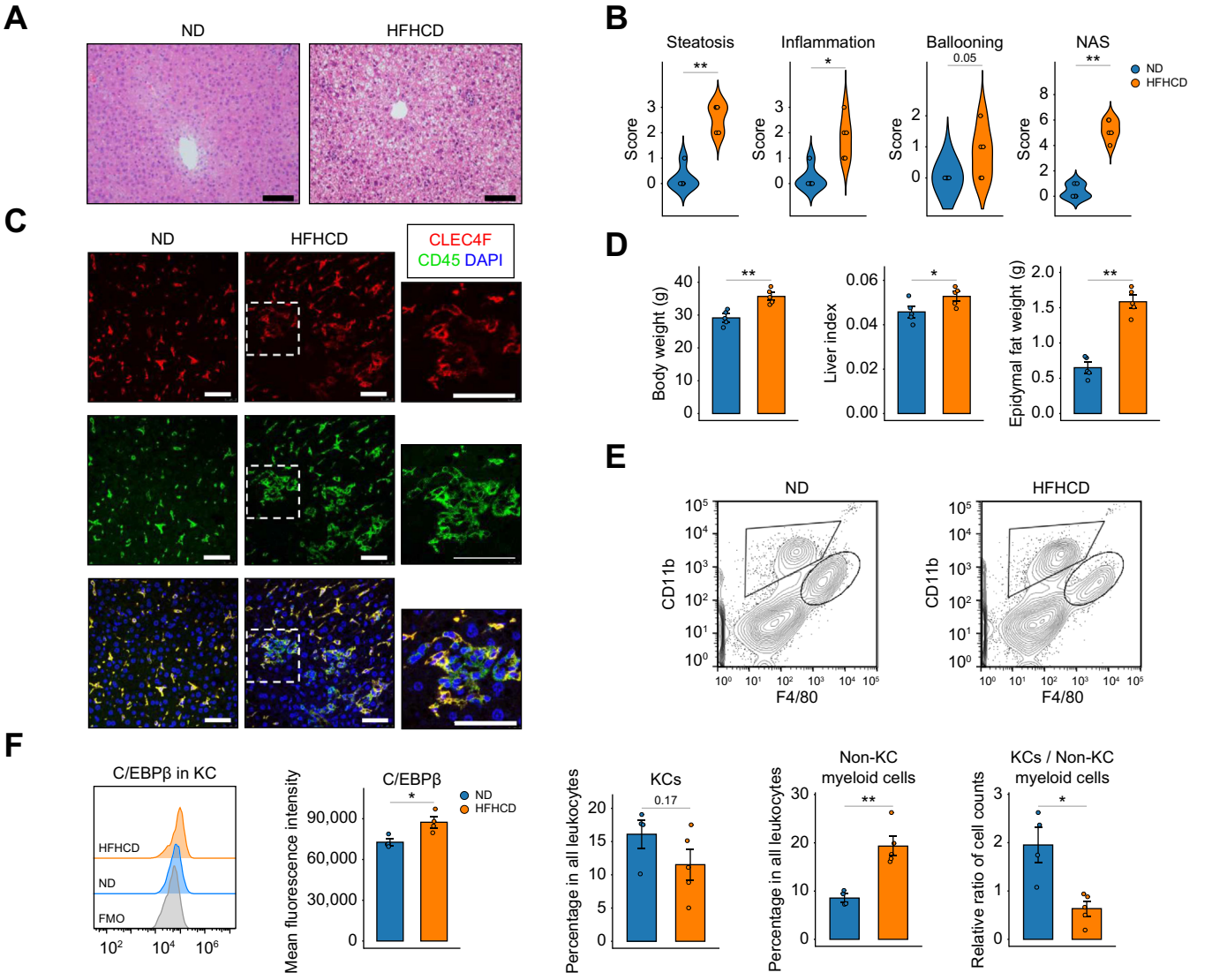

Fig. 1. Presence of hepatic inflammation and changes in hepatic macrophages in the HFHCD-induced MASLD model. (A and B) Representative H&E staining (A) (scale bar = 100 μm) and NAS score (B) based on liver sections. (C) Body weight, liver index (the ratio of liver weight to body weight), and epidymal fat weight at Week 12 (n = 5 for each group). (D) Representative immunofluorescence images showing the distribution of CLEC4F and CD45 in liver sections (scale bar = 50 μm). (E) Flow cytometry analysis of KCs and non-KC myeloid cells from ND and HFHCD mice with relative quantification (n = 4 for the ND group and n = 5 for the HFHCD group). (F) Intracellular flow cytometry analysis showing the protein level of C/EBPβ in KCs (n = 4 for each group). Results were compared by Wilcoxon Rank Sum test (B) or unpaired two-tailed Student's t-test (D-F). Bars represent mean ± SEM. *p <0.05, **p <0.01. C/EBPβ, CCAAT/enhancer binding protein β; HFHCD, high-fat and high-cholesterol diet; KC, Kupffer cell; MASLD, metabolic dysfunction-associated steatotic liver disease; ND, normal diet.

specific *Cebpb* monoallelic knockout caused a significant decrease in C/EBPβ protein level in KCs, but not in non-KC myeloid cells (Fig. S2B), indicating that KC-specific *Cebpb* monoallelic knockout can effectively knock down *Cebpb* in KCs. In ND-fed mice, KC-specific *Cebpb* knockdown did not alter VSIG4 expression and the cell number of KCs, indicating an unchanged KC pool (Fig. S2C and D). Histological analysis and metabolic indices were also not changed (Fig. S2E and F). In HFHCD-fed mice, KC-specific *Cebpb* knockdown significantly reduced intralobular inflammation and NAS score, although the steatosis and ballooning were not significantly altered (Fig. 2A and B). Immunofluorescence further verified the reduction in KC-related inflammatory foci after knockdown (Fig. 2C–E). Meanwhile, liver enzymes, as well as metabolic indices and liver triglyceride content, were not significantly altered (Fig. S3A–D). We further evaluated numeric changes in hepatic macrophage subsets. Although KC-specific *Cebpb* knockdown did not significantly alter the relative proportion of EmKCs within the KC pool (Fig. 2F and Fig. S3E), it contributed to a significant increase in the overall KC proportion and decrease in non-KC myeloid cells within the hepatic leukocyte pool, as well as a prominent increasing trend in KC/non-KC myeloid cell ratio (p = 0.06) (Fig. 2G). These results collectively indicate that C/EBPβ in KCs mainly plays a promotive role in inflammatory immune cell infiltration into the liver in MASLD.

We then used RNA-seq to further explore the effect of KC-specific *Cebpb* knockdown in MASLD (Fig. 3A). KC-specific *Cebpb* knockdown induced significant transcriptomic changes in the MASLD liver, most of which were down-regulated differentially expressed genes (DEGs) (Fig. 3B). For

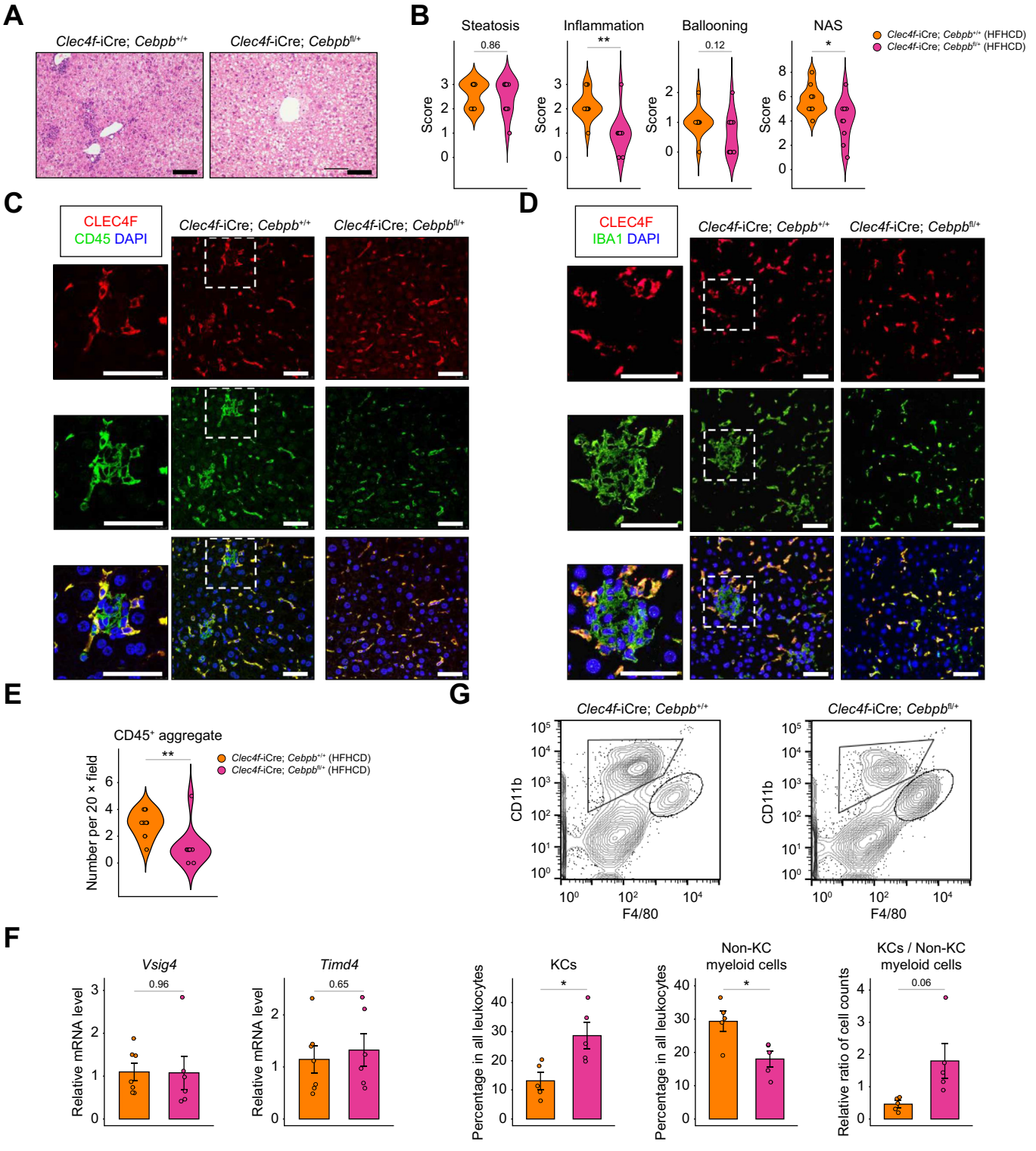

Fig. 2. KC-specific *Cebpb* knockdown alleviates hepatic inflammation in MASLD. (A and B) Representative H&E staining (A) (scale bar = 100 μm) and NAS score (B) based on liver sections (n = 10 for each group from two independent experiments). (C–E) Representative immunofluorescence images of liver sections showing the distribution of CLEC4F and CD45 (C) and CLEC4F and IBA1 (D) (scale bar = 50 μm); the number of $CD45^+$ leukocyte aggregates per 20 × field was additionally counted (E). (F) Relative mRNA levels of EmKC marker genes in livers. (G) Flow cytometry analysis of KCs and non-KC myeloid cells with relative quantification (n = 5 for each group). Results were compared by Wilcoxon Rank Sum test (B, E) or unpaired two-tailed Student's t-test (F, G). Bars represent mean ± SEM. *p <0.05, **p <0.01. EmKC, embryonic KC; HFHCD, high-fat and high-cholesterol diet; KC, Kupffer cell; MASLD, metabolic dysfunction-associated steatotic liver disease.

immune cell marker genes that were identified according to murine scRNA-seq data (Fig. S4A), we found that genes in the "Monocyte/MoMFs only," "KCs and Monocyte/MoMFs," and "Neutrophils only" myeloid cell marker sets, as well as in the "pan-T cells" and "CD8$^+$ T cells" lymphocyte marker sets, were uniformly downregulated by knockdown (Fig. S4B and C). Gene ontology (GO) functional enrichment of DEGs revealed that the downregulated DEGs were mainly related to "leukocyte migration/chemotaxis" and "monocyte/granulocyte/neutrophil migration/chemotaxis" in GO "biological processes" (Fig. 3C) and "cytokine receptor binding" and "transmembrane signaling receptor/cytokine receptor/immune receptor activity" in GO "molecular function" (Fig. S4D). Using reverse transcription quantitative PCR (RT-qPCR), we verified significantly decreased expression of CD8$^+$ T-cell, MoMF, and neutrophil markers induced by KC-specific *Cebpb* knockdown in the liver (Fig. 3E). Decreased infiltration of CD8$^+$ T cells and neutrophils was further verified by immunofluorescence staining (Fig. 3F–H). We then focused on the "leukocyte migration" term and found that pertinent downregulated DEGs include multiple genes encoding multiple cytokines/chemokines and cell adhesion molecules (Fig. S4E).

Together, these results suggest that C/EBPβ in KCs promotes the infiltration of immune cells, including MoMFs, neutrophils, and CD8$^+$ T cells in hepatic inflammation in MASLD, and that the underlying molecular mechanism might involve leukocyte migration-related mechanisms.

Increased C/EBPβ activity in MASH selectively modulates pathogenic transcriptional regulatory network in KCs

C/EBPβ in KCs was predominantly localized in the cell nucleus (Fig. 4A), suggesting a close relationship between C/EBPβ and transcriptional regulation in KCs. To determine the binding sites of C/EBPβ in the KC genome, we performed C/EBPβ CUT&Tag-seq in sorted KCs. C/EBPβ CUT&Tag signals were enriched in genomic areas around transcription start sites (TSSs), and the overall signal intensity of C/EBPβ in TSS-adjacent regions was higher in KCs from HFHCD-fed mice (Fig. 4B). We then evaluated the overall correlation between C/EBPβ CUT&Tag signals and ChIP-seq (LXR, ATF3, and p300) or ATAC-seq signals in KCs. We found relatively high correlations among C/EBPβ, ATF3, and p300 signals (ρ = 0.51–0.84), as well as between LXR and ATAC signals (ρ = 0.59–0.60), whereas the correlations between C/EBPβ/ATF3/p300 and LXR/ATAC were relatively low (ρ = 0.11–0.54) (Fig. 4C). In addition, among C/EBPβ/ATF3/p300, the correlations between samples from MASLD KCs were higher than those between samples from control KCs (Fig. 4C). These results indicate that C/EBPβ is a MASLD-associated stimulus-regulated TF and is closely related to ATF3/p300-mediated pathogenic transcriptional regulation.

To unravel the influence of dynamic changes in C/EBPβ distribution on KC transcriptomic changes during MASLD pathogenesis, we classified C/EBPβ CUT&Tag signal peaks into three sets according to MASLD-induced changes in C/EBPβ signal intensity (Fig. S5A). A high level of ATAC signal in the "upregulated" and "non-altered" peak sets (Fig. S5B) indicated their high potential in transcriptional regulation, which attracted our attention. Nearly half of the C/EBPβ "upregulated" peaks were enriched in promoter regions, whereas this proportion was lower for "non-altered" peaks (Fig. 4D). In addition, we observed the relationship between MASLD-induced DEGs in KCs[15] (Fig. S5C) and further subclassified the C/EBPβ "upregulated"/"non-altered" peaks in promoter regions according to signal intensity (Fig. S5D). We found that the C/EBPβ promoter peak sets exhibited larger overlap with the promoters of MASLD-induced upregulated DEGs compared with downregulated DEGs. Moreover, the C/EBPβ "upregulated" "high-intensity" promoter peak set had the largest overlap with MASLD-induced upregulated DEGs (n = 112) (Fig. 4E). We also found that there was *de facto* distribution of ATF3 or p300 in C/EBPβ peak regions and the ATF3 or p300 ChIP signal intensity in the C/EBPβ "high-intensity" peak sets was higher than that in the C/EBPβ "low-intensity" peak sets (Fig. 4F). Furthermore, although MASLD induced an overall increase in ATF3 or p300 signal intensity (Fig. S5E), the fold of increase in the C/EBPβ "low-intensity" "non-altered" peak set was significantly lower than that in the other three peak sets, and the fold of increase in the C/EBPβ "low-intensity" "upregulated" peak set was significantly lower than that in the "high-intensity" "upregulated" peak set (Fig. 4F and G), indicating a potential role of C/EBPβ in selectively promoting ATF3/p300-mediated pathogenic transcriptional regulation.

Collectively, these results indicate that C/EBPβ activity is increased in KCs in MASLD, leading to a selectively promotive effect on the promoters of MASLD-induced genes synergistically with other stimulus-regulated factors, including ATF3 and p300.

C/EBPβ in KCs promotes cellular VCAM1 expression in MASH pathogenesis

To screen for direct downstream genes influenced by increased C/EBPβ activity in KCs, we performed an integrated analysis of the "upregulated" peaks of C/EBPβ CUT&Tag-seq data in KCs and RNA-seq data in the liver. Overall, KC-specific *Cebpb* knockdown exerted a significant suppressive effect on the hepatic transcriptome in MASLD (Fig. 5A). For specific downstream genes, the top five predicted suppressed genes were *Lyz2*, *Vcam1*, *Pla2g7*, *Parvg*, and *CCl6* (Fig. 5A). According to murine scRNA-seq data, *Vcam1* was predominantly highly expressed in KCs but not in other cells in the murine MASLD liver (Fig. 5B). In addition to high expression in KCs, a moderate level of *Vcam1* expression could only be found in liver sinusoidal endothelial cells (LSECs) (Fig. 5B). Therefore, KCs can be regarded as the main cellular source of *Vcam1* transcripts in the hepatic transcriptome, and the KC-specific *Cebpb* knockdown-induced decrease in hepatic *Vcam1* expression is highly likely to be attributed to C/EBPβ-mediated transcriptional activation in KCs.

The protein encoded by *Vcam1* is vascular cell adhesion molecule 1 (VCAM1), a cell adhesion molecule that facilitates inflammation-related vascular adhesion of leukocytes.[22] Considering the close relationship between VCAM1 and inflammation, we further focused on the potential influence of C/EBPβ on *Vcam1* expression in KCs. A significant decrease in the hepatic mRNA level of *Vcam1 per se*, as well as *Itga4* and *Itgb7* (genes encoding VCAM1 ligands integrin α4 and β7, respectively), was verified using RT-qPCR (Fig. 5C). In addition, there was a prominent C/EBPβ CUT&Tag signal peak in the *Vcam1* exon 1 region of KCs from MASLD mice (Fig. 5D). This

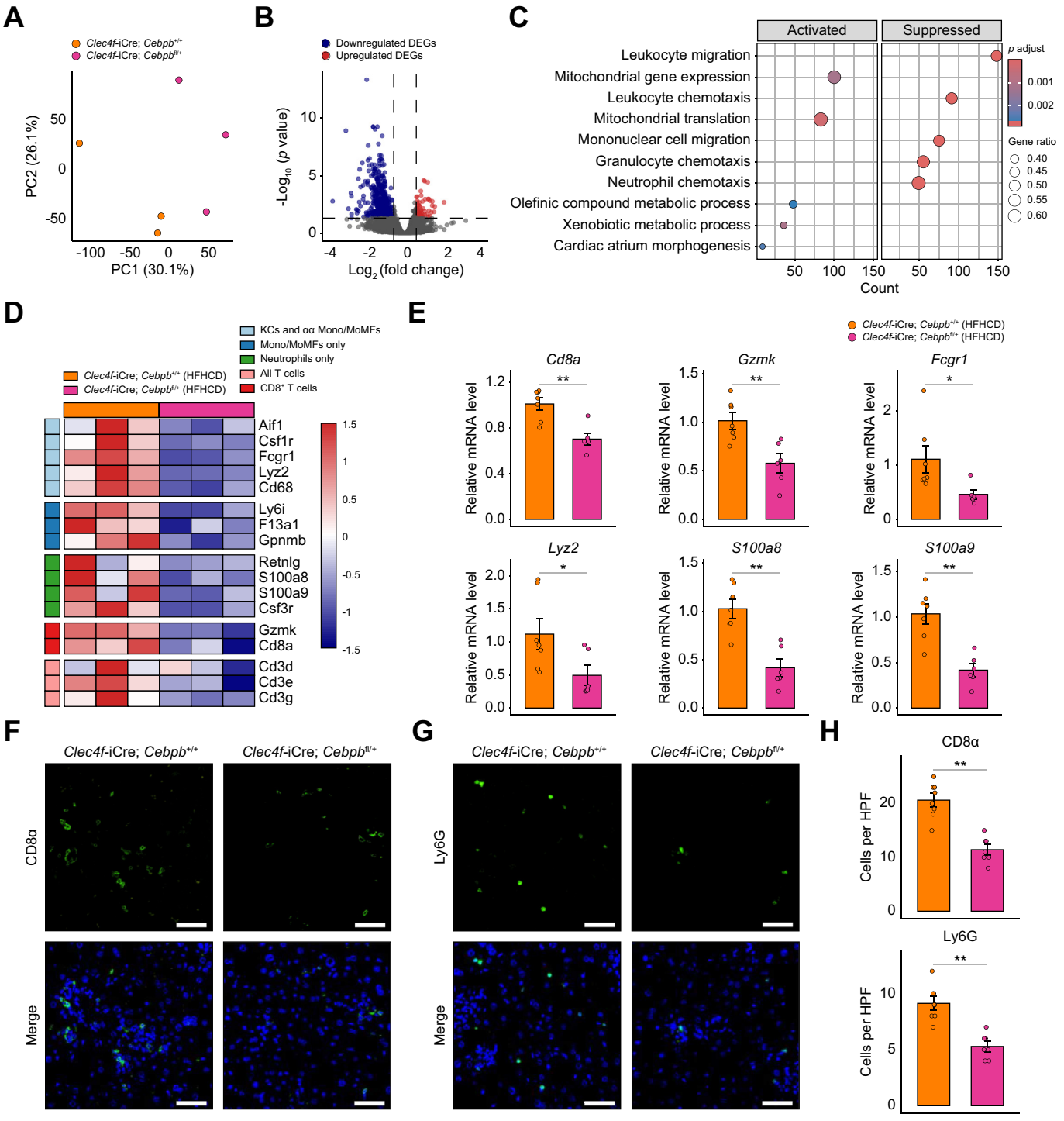

Fig. 3. KC-specific *Cebpb* knockdown reduces hepatic immune cell infiltration by inhibiting leukocyte migration in MASLD. (A–D) RNA-seq was performed on RNA isolated from liver tissue (n = 3 for each group). (A) Principal component analysis. (B) Volcano plot showing upregulated/downregulated DEGs between two groups. (C) Top 10 GO biological processes in GSEA analysis of DEGs. (D) Heatmap showing indicated cell subset marker expression. (E) Relative mRNA levels of hepatic immune cell marker genes in livers. (F–H) Representative immunofluorescence images of liver sections showing the distribution of CD8α (F) and Ly6G (G) with quantification of $CD8\alpha^+$ or $Ly6G^+$ cells per high-power field (HPF) (H) (scale bar = 50 μm). Results were compared using unpaired two-tailed Student's *t* test; n = 7 for the *Clec4f*-iCre;*Cebpb*$^{+/+}$ group and n = 6 for the *Clec4f*-iCre;*Cebpb*$^{fl/+}$ group. Bars represent mean ± SEM. **p* <0.05, ***p* <0.01. DEG, differentially expressed gene; GO, gene ontology; GSEA, gene set enrichment analysis; HFHCD, high-fat and high-cholesterol diet; KC, Kupffer cell; MoMF, monocyte-derived macrophage; PC, principal component.

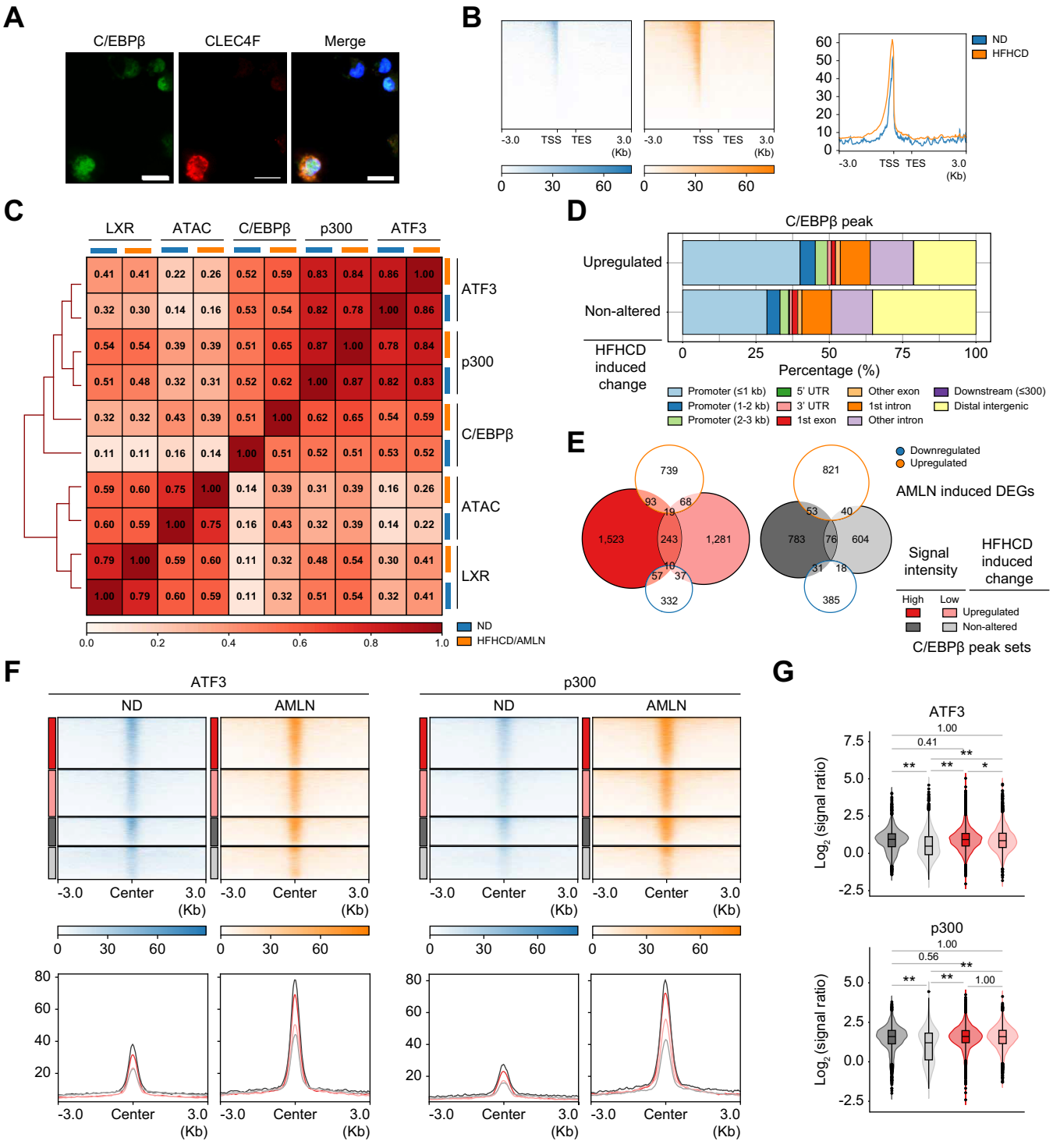

Fig. 4. C/EBPβ activity in KCs is increased in MASLD and mediates selective modulation of ATF3/p300-related transcriptional regulation. (A) Immunofluorescence showing the intracellular distribution of C/EBPβ (green) in murine liver immune cells (scale bar = 10 μm). (B) Average enrichment heatmap and profile of C/EBPβ CUT&Tag signals around genic regions. (C) Spearman correlation heatmap with hierarchical clustering showing the correlation in overall genomic distribution between C/EBPβ CUT&Tag signals and ChIP-seq (LXR, ATF3, and p300) or ATAC-seq signals. (D) Barplot of C/EBPβ CUT&Tag peak distribution in genomic features. (E) Venn plots showing the overlaps between AMLN-induced upregulated/downregulated DEGs and four gene sets annotated from C/EBPβ peak sets in promoter regions. (F) Average enrichment heatmap and profile of ATF3 and p300 signals ± 3 kb around four C/EBPβ peak sets. (G) Log ratio of ATF3 and p300 ChIP-seq signal (AMLN *vs*. ND) at four C/EBPβ peak sets. Results were compared using Dunn's test after the Kruskal–Wallis test (G). **p* <0.05, ***p* < 0.01. C/EBPβ, CCAAT/enhancer binding protein β; DEG, differentially expressed gene; HFHCD, high-fat and high-cholesterol diet; KC, Kupffer cell; MASLD, metabolic dysfunction-associated steatotic liver disease; ND, normal diet.

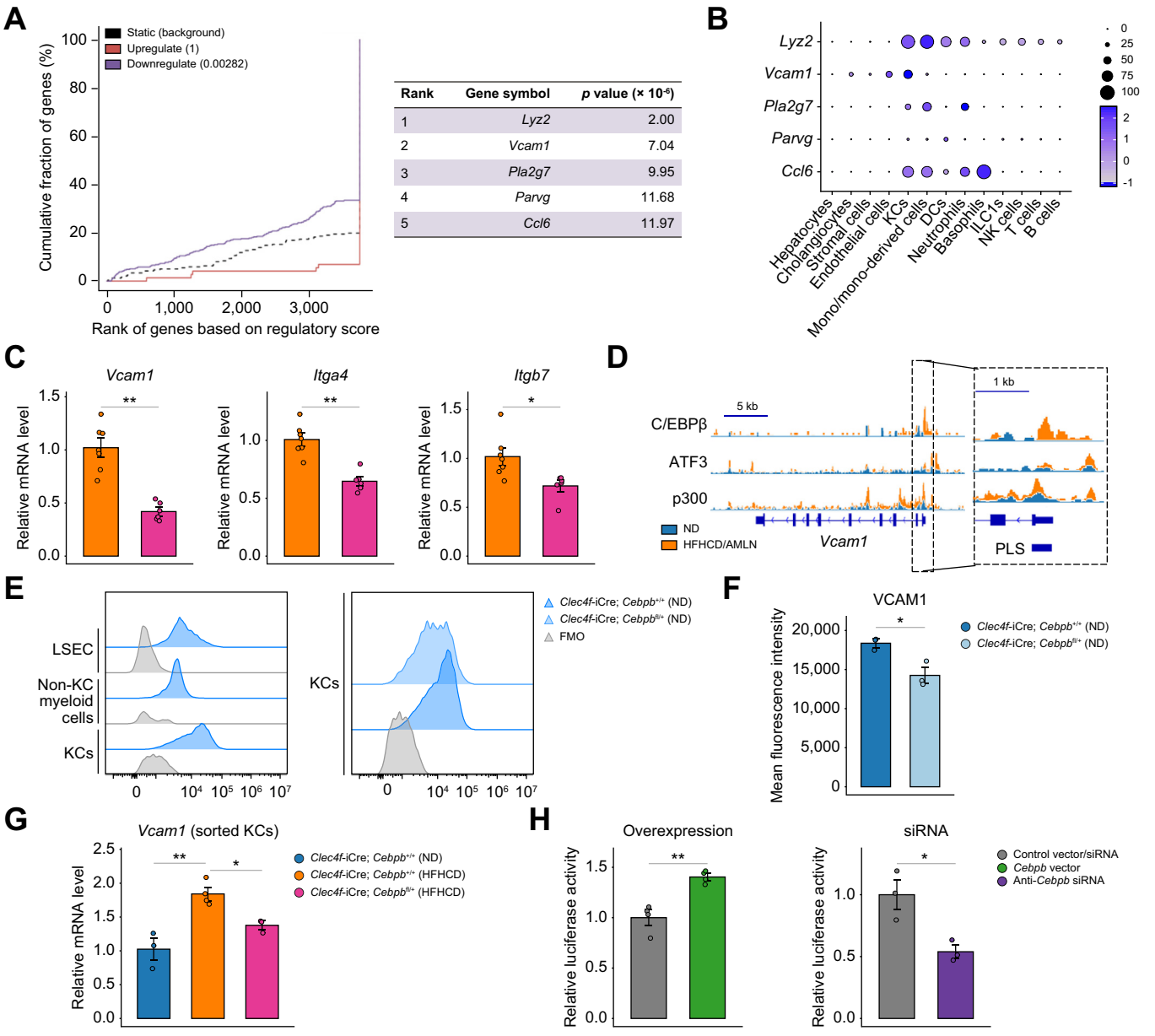

Rank	Gene symbol	*p* value (× 10⁻⁶)
1	*Lyz2*	2.00
2	*Vcam1*	7.04
3	*Pla2g7*	9.95
4	*Parvg*	11.68
5	*Ccl6*	11.97

Fig. 5. C/EBPβ-mediated transcriptional activation promotes the expression of VCAM1 in KCs of MASLD mice. (A) Activating/repressive function prediction of HFHCD-induced upregulated C/EBPβ peaks in KCs from MASLD mice, with the top five genes in prediction. (B) Expression of indicated genes in scRNA-seq of murine MASLD liver. (C) Relative mRNA levels of indicated genes in the liver. (D) Representative genomic track showing C/EBPβ, ATF3, and p300 distribution at the *Vcam1* gene loci in KCs. (E and F) Flow cytometry analysis of the VCAM1 protein level (E) with quantification (F) (n = 3 for each group). (G) Relative mRNA level of *Vcam1* in sorted KCs (n = 4 for the "*Clec4f*-iCre;*Cebpb*$^{+/+}$ HFHCD" group and n = 3 for the other two groups). (H) Relative luciferase activity of the *Vcam1* promoter in AML12 cells transfected with murine C/EBPβ overexpression plasmid (left panel, n = 4 for each group) or siRNA targeting C/EBPβ (right panel, n = 3 for each group). Results were compared using an unpaired two-tailed Student's *t* test (C, F, and H) or one-way ANOVA and least significant difference (LSD) *post hoc* test (G). Bars represent mean ± SEM. **p* <0.05, ***p* <0.01. C/EBPβ, CCAAT/enhancer binding protein β; HFHCD, high-fat and high-cholesterol diet; KC, Kupffer cell; MASLD, metabolic dysfunction-associated steatotic liver disease; ND, normal diet.

region was annotated as the *Vcam1* promoter region according to the ENCODE candidate CRE and possessed MASLD-induced increased distribution of ATF3 and p300 (Fig. 5D). FCM analysis showed that KCs expressed the highest protein level of VCAM1 in murine non-parenchymal cells, and *Cebpb* knockdown sufficed to induce a decrease in the VCAM1 protein level in KCs (Fig. 5E and F). In addition, the HFHCD-induced increase in *Vcam1* expression in KCs was significantly reversed by *Cebpb* knockdown (Fig. 5G). To further validate the C/EBPβ-mediated transcriptional activation effect on the murine *Vcam1* promoter, we performed dual-luciferase reporter assays. We found that overexpression and siRNA knockdown of *Cebpb* significantly promoted and inhibited the transcriptional activity of the *Vcam1* promoter, respectively (Fig. 5H), indicating a promotive effect of C/EBPβ on *Vcam1* promoter activity. In summary, these results suggest that C/

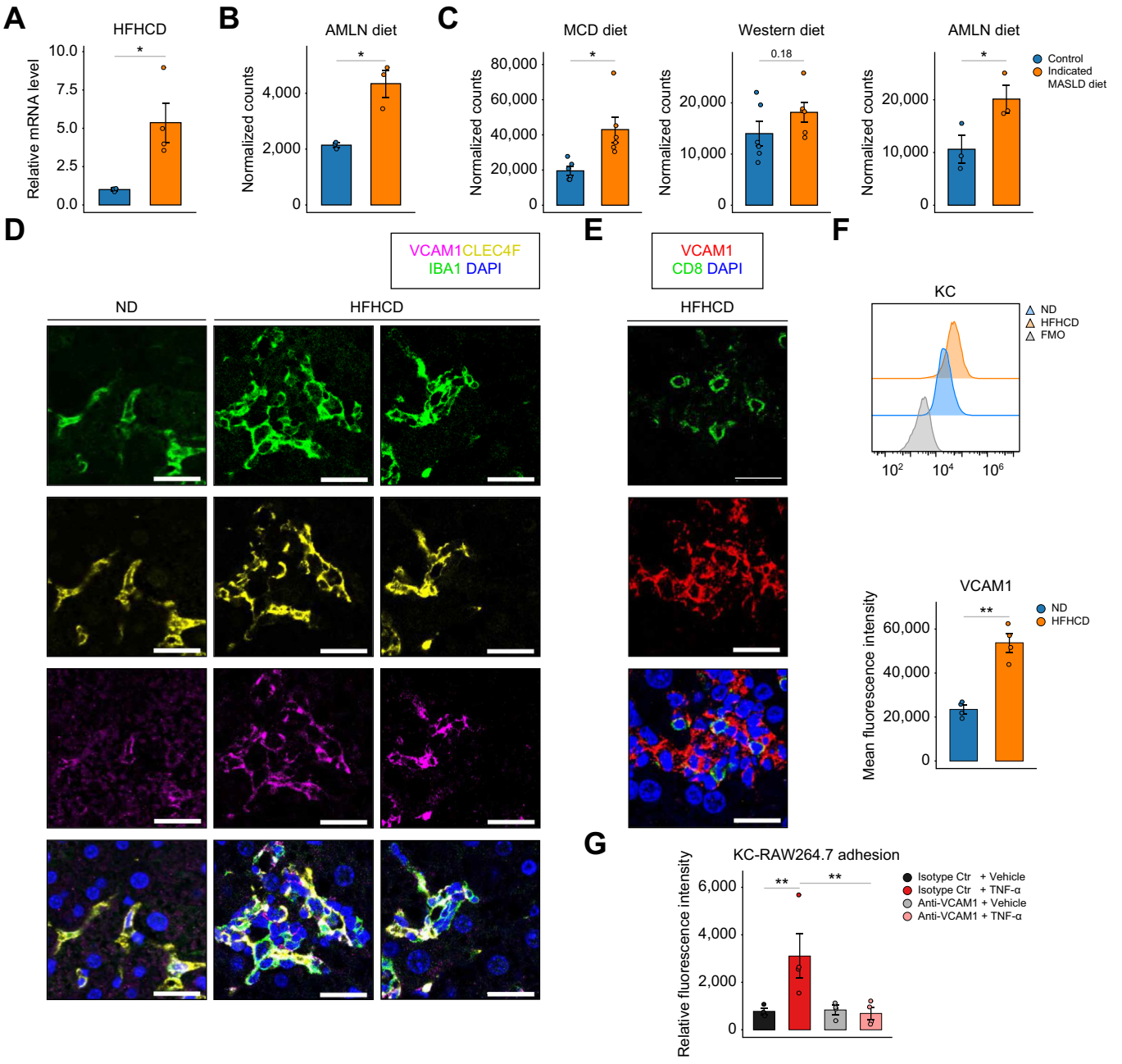

Fig. 6. KC-expressed VCAM1 is upregulated and promotes immune cell infiltration in MASLD. (A, D–F) Wild-type C57BL/6J mice were administered with HFHCD or ND. (A) Relative mRNA levels of *Vcam1* in liver tissue. (D and E) Representative immunofluorescence images of liver sections showing the distribution of VCAM1 with CLEC4F and IBA1 (D), and VCAM1 with CD8α (E) (scale bar = 20 μm). (F) Flow cytometry analysis showing the VCAM1 protein level in KCs. (B and C) *Vcam1* expression in RNA-seq of liver tissue (B) or FCM-sorted KCs (C) from mice in different dietary MASLD models. (G) Cell adhesion assay *in vitro* showing the adhesion of RAW264.7 cells to murine primary KCs after administration of murine TNF-α and/or anti-VCAM1 antibody. Results were compared using an unpaired two-tailed Student's *t* test (A, F) or one-way ANOVA and an LSD *post hoc* test (G). Bars represent mean ± SEM. *p <0.05, **p <0.01. HFHCD, high-fat and high-cholesterol diet; KC, Kupffer cell; MASLD, metabolic dysfunction-associated steatotic liver disease; ND, normal diet.

EBPβ in KCs can bind to the *Vcam1* promoter, leading to increased *Vcam1* promoter activity and *Vcam1* gene expression in MASLD.

VCAM1 in KCs is overexpressed and promotes hepatic inflammation in MASH

To explore the role of KC-expressed VCAM1 in MASLD pathogenesis, we first observed *Vcam1* expression in the liver tissue of MASLD mice. We found that both the HFHCD and Amylin liver NASH (AMLN) diets could significantly promote *Vcam1* expression in liver tissue (Fig. 6A and B). We also analyzed RNA-seq data of FCM-sorted KCs from MASLD mice. We found that *Vcam1* expression in KCs was significantly increased by the methionine-choline deficient diet (MCD) or AMLN diet, or exhibited an increasing trend in mice fed a Western diet (Fig. 6C). We then assessed the spatial

distribution of VCAM1 in the murine MASLD liver. We found that VCAM1 was intensely distributed in the inflammatory foci of the livers of HFHCD-fed mice and co-localized with CLEC4F$^+$ IBA1$^+$ KCs, whereas it was weakly distributed in the livers of ND-fed mice and colocalized with KCs (Fig. 6D). In addition, CLEC4F$^-$ IBA1$^+$ MoMFs and CD8$^+$ T cells were also detected in these inflammatory foci, in direct physical interaction with VCAM1$^+$ KCs (Fig. 6D and E). In addition, similar to changes in the *Vcam1* mRNA level in KCs, FCM analysis showed that HFHCD significantly increased the VCAM1 protein level in KCs (Fig. 6F). To verify the role of KC-expressed VCAM1 in leukocyte infiltration, we detected RAW264.7 cell adhesion to primary KCs with increased (TNF stimulation) or blocked (anti-VCAM1 administration) VCAM1 *in vitro*. We found that RAW264.7 cell adhesion to primary KCs was significantly increased after TNF stimulation, and this increase could be significantly abrogated by anti-VCAM1 administration (Fig. 6G). Together, these results suggest that KC-expressed VCAM1 is upregulated in MASLD pathogenesis, and participates in the inflammatory infiltration of immune cells such as MoMFs and CD8$^+$ T cells in MASLD.

Upregulated VCAM1 in KCs is implicated in human MASH pathogenesis

To verify the involvement of KC-expressed VCAM1 in human MASLD pathogenesis, we first observed the hepatic mRNA level of VCAM1 in RNA-seq data of patients with biopsy-proven MASLD. We found that VCAM1 expression in the liver tissue of patients with MASL and MASH was significantly higher than that in healthy controls in one dataset (GSE61260) (Fig. 7A). In another dataset (GSE135251), VCAM1 expression also exhibited an increasing trend in the liver tissue of patients with MASL and early MASH (F0-1) compared with healthy controls (Fig. 7A). Furthermore, in a microarray analysis dataset (GSE106737) comparing the liver transcriptome of patients with MASLD before and after treatment, hepatic VCAM1 expression was significantly decreased in patients with MASLD responding effectively to lifestyle intervention (LI) or exhibited a decreasing trend in patients with MASLD receiving Roux-en-Y gastric bypass (RYGB). In contrast, it was not significantly altered in patients with MASLD responding ineffectively to LI (Fig. 7B), indicating a close relationship between hepatic VCAM1 and MASLD prognosis.

We then examined the spatial distribution of VCAM1 in healthy human and MASH liver. We found that VCAM1 was sparsely distributed in healthy human liver, whereas it was predominantly distributed in the immune cell aggregates of MASH patient liver (Fig. 7C). Nonetheless, the VCAM1 signal in both healthy and MASH liver was co-localized with IBA1$^+$ macrophages in the inflammatory foci (Fig. 7C). Accordingly, *VCAM1* was predominantly highly expressed in KCs and exhibited a higher expression level in KCs of patients with >10% steatosis in human liver scRNA-seq (Fig. 7D). In addition, overexpression of human *CEBPB* significantly promoted transcriptional activity of the *VCAM1* promoter (Fig. 7E), verifying the promotive effect of C/EBPβ on *VCAM1* promoter activity in human cells.

Discussion

Hepatic inflammation in MASLD is a key pathogenic process for further disease progression into advanced liver diseases. It involves complicated interactions among multiple types of cells and molecules in the liver microenvironment, and can be partially independent from pathological changes in hepatocytes, such as steatosis or necrosis.[3,4] However, further details in its pathogenesis are complicated and remain elusive till now. Dysregulations in KC phenotype and function have long been regarded as key pathogenic mechanisms in MASLD.[23,24] In our present study, we provide robust evidence to support the essential role of KC dysregulation in hepatic inflammation in MASLD. We identified C/EBPβ in KCs as a key pathogenic factor that promotes hepatic inflammation by selectively activating the pathogenic transcriptional regulatory network in KCs. We further found that MASLD-induced increased C/EBPβ activity promoted VCAM1 expression in KCs by activating the *Vcam1* promoter, leading to subsequent immune cell infiltration in murine MASLD. The discovery of the proinflammatory "C/EBPβ/VCAM1" axis in KCs promises to update current understanding in KC biology and MASLD pathophysiology, and provide insights into targeted intervention and treatment in MASLD.

Dynamic changes in hepatic macrophages during MASLD pathogenesis have always been the research focus. Although it is acknowledged that the KC number remains relatively constant or decreases and the MoMF number significantly increases in MASH,[10,12,25] the specific role (pathogenic or protective) of each macrophage subset remains controversial.[25–29] In this study, in addition to similar changes in macrophage subset numbers, we found that KCs (both EMKCs and MoKCs) were in close contact with infiltrating immune cells in hepatic inflammation in MASLD (Fig. 1), and hepatic inflammation in MASLD could be alleviated by KC-specific *Cebpb* knockdown (Figs 2 and 3), indicating the existence of KC-mediated pathogenic effect in hepatic inflammation in MASLD. It is undeniable that KC can play a protective role in MASLD pathogenesis by clearing necroptotic hepatocytes or ameliorating metabolism-related oxidative stress.[29,30] However, KCs can also exacerbate MASLD in a proinflammatory manner.[31,32] Together with our findings, KCs, the seemingly "victims" in terms of numeric decline during MASLD, are complex and multifaceted in MASLD pathogenesis, possessing both pathogenic and protective functions. Correspondingly, targeting the pathogenic aspect of KCs is a potential strategy for precise intervention of hepatic inflammation in MASLD.

Therapeutic targets of KCs in MASLD have been scarcely explored. Candidate molecules may include MSR1 and MiT/TFE, according to previous studies.[31,32] There have been studies indicating a pathogenic role of C/EBPβ in MASLD. *Cebpb* global knockout and bone marrow transplantation-mediated "immune-specific" *Cebpb* knockout have been found to alleviate systemic metabolic disorders, hepatic steatosis, and liver injury in MASLD mice.[33–36] Taking advantage of the Cre-loxP system, we shrank the cell types subjected to intervention, focusing on C/EBPβ function in one specific subset of hepatic macrophages, namely, KCs. We found an abnormal elevation of C/EBPβ levels in KCs (Fig. 1) and the therapeutic effect of KC-specific *Cebpb* knockdown in hepatic inflammation in MASLD (Figs 2 and 3), thus verifying the pathogenic role of C/EBPβ in KCs. Similarly, *Cebpb* knockdown (monoallelic knockout) in microglia (brain tissue-resident macrophages) could help alleviate brain inflammation in chronic neurodegenerative diseases,[37,38] indicating the therapeutic

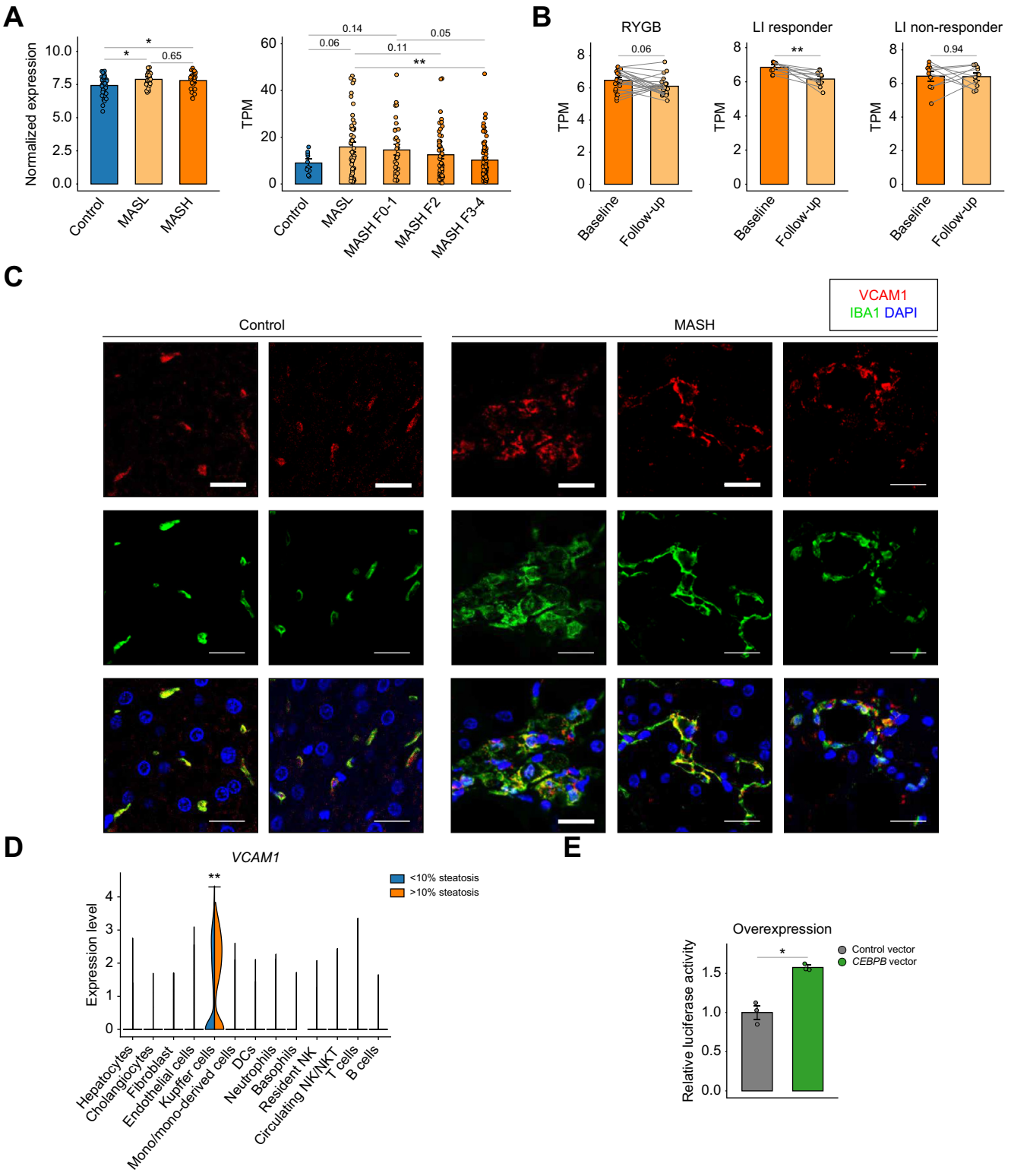

Fig. 7. Increased VCAM1 in KCs is associated with hepatic inflammation in patients with MASH. (A and B) VCAM1 expression in RNA-seq of liver tissue from patients with MASLD or healthy controls (A) and patients with MASH before and after RYGB or LI (B). (C) Representative immunofluorescence images of VCAM1 and IBA1 (C) in liver sections of patients with MASH or healthy controls (scale bar = 20 μm). (D) Expression of *VCAM1* in liver scRNA-seq of patients with different hepatic steatosis degrees. (E) Relative luciferase activity of the *VCAM1* promoter in HUVECs transfected with human C/EBPβ overexpression plasmid or control plasmid (n = 3 for each group). Results were compared using one-way ANOVA and an LSD *post hoc* test (A), a paired two-tailed Student's *t* test (B), Wilcoxon rank sum test (D), or an unpaired two-tailed Student's *t* test (E). Bars represent mean ± SEM. **p* <0.05, ***p* <0.01. C/EBPβ, CCAAT/enhancer binding protein β; HUVEC, human umbilical vein endothelial cell; KC, Kupffer cell; LI, lifestyle intervention; MASL, metabolic dysfunction-associated steatotic liver; MASH, metabolic dysfunction-associated steatohepatitis; MASLD, metabolic dysfunction-associated steatotic liver disease; RYGB, Roux-en-Y gastric bypass.

effect of C/EBPβ knockdown. In addition, from the perspective of the overall MASLD pathophysiology, MASLD is characterized by metabolic inflammation,[39] whereas C/EBPβ is well known for its dual involvement in metabolic and immune dysregulations.[17,19] Therefore, metabolic inflammation in the MASLD liver microenvironment may induce increased C/EBPβ levels and activity in KCs, leading to abnormally altered KC functions and sequentially exacerbated hepatic inflammation. Collectively, C/EBPβ in KCs is a promising new therapeutic target for treating MASLD-related hepatic inflammation.

To adapt to different tissue microenvironments, transcriptional regulatory networks vary among different types of macrophages, as exemplified by differences in lineage-determining TFs among different tissue-resident macrophages.[40,41] In the era of KC biology, LXR and ATF3 have been identified as lineage-determining TFs and MASLD-associated stimulus-regulated TFs in KCs. However, the transcriptional regulatory network of KCs has not been fully elucidated. One key highlight of our study is the comprehensive profiling of C/EBPβ genomic distribution in KCs of different states *in vivo*. In our study, we identified C/EBPβ in KCs as a new MASLD-associated stimulus-regulated TF that selectively promotes ATF3/p300-mediated transcriptional activation in MASLD (Fig. 4). In previous studies on non-KC macrophages (*e.g.* alveolar macrophages and monocyte-derived macrophages), C/EBPβ was regarded as a lineage-determining TF for maintaining cell identity.[18,42] In contrast, our findings indicate a different role of C/EBPβ in KCs, which may stem from differences in the overall composition of the transcriptional regulatory network. Nevertheless, our findings provide a deeper understanding of the transcriptional regulatory network of KCs.

The molecular mechanism of immune cell infiltration into the liver in MASLD is complex and has not been fully elucidated.[3,4] VCAM1 is an endothelial cell-expressed cell surface glycoprotein that can promote leukocyte adhesion and migration across the vascular wall via ligand–receptor interaction with integrin, thereby promoting the infiltration of immune cells in pathological states.[22,43] In MASLD-related studies, VCAM1 was found to be highly expressed in the MASLD liver, and antibody treatment targeting VCAM1 or its ligand integrin α4β7 in MASLD mice can significantly improve liver inflammation in mice.[44,45] In our study, we found a positive correlation between KC-expressed VCAM1 and hepatic inflammation in MASLD (Figs 6 and 7). More importantly, we found that increased C/EBPβ activity in the *Vcam1* promoter promotes *Vcam1* expression in KCs in MASLD, thus promoting KC-mediated immune cell infiltration by "VCAM1–Integrin α4" interaction (Figs 5 and 6). VCAM1 has been found to be expressed in tissue-resident macrophages, including splenic macrophages and KCs,[46] in addition to endothelial cells. However, the physiological and pathophysiological roles of macrophage-expressed VCAM1 have been scarcely reported. A previous study found that KC-expressed VCAM1 may participate in extramedullary erythrocyte hematopoiesis in liver.[47] Therefore, we propose that VCAM1 in KCs is expressed at a relatively low level for homeostasis-related functions under physiological conditions, but the abnormally high expression of VCAM1 in KCs (induced by C/EBPβ and/or other factors) would contribute to hepatic inflammation under pathological conditions such as MASLD. Furthermore, upregulation of VCAM1 expression has long been attributed to pathological activation of the TNF-α/NF-κB signaling pathway according to previous studies in endothelial cells.[43] Considering the previous report of the interaction between C/EBPβ and NF-κB-related proteins,[19] C/EBPβ in KCs is likely to play a synergistic role with the NF-κB signaling pathway to promote *Vcam1* expression. Meanwhile, given that VCAM1 plays an important role in physiological processes such as hemopoietic stem cells homing in the hematopoietic microenvironment,[48,49] targeted intervention of the C/EBPβ/VCAM1 axis in KCs may be superior to systemic interventions such as anti-VCAM1 injection in terms of efficacy and safety.

The main limitation of this study is the absence of direct transcriptome analysis of sorted KCs, thus influencing the efficacy of screening for more downstream genes of C/EBPβ in KCs. This is mainly a result of our technology limitations in KC isolation and RNA extraction, as well as the relatively high requirement of RNA input for RNA-seq. We also failed to make a deeper exploration of the molecular mechanism owing to the difficulty in DNA/RNA transfection to macrophages and the unavailability of a large quantity of primary murine KCs. In addition, we did not make a detailed subclassification of hepatic macrophages in the murine MASLD liver. For a thorough evaluation of the hepatic inflammation landscape, further subclassification of F4/80^{int} CD11b^{hi} leukocytes, as well as identification of some newly recruited F4/80^{int} CD11b^{hi} MoKCs among these cells, should be considered in future studies. Likewise, discrimination between EmKCs and MoKCs (based on TIMD4 expression) among F4/80^{hi} CD11b^{int} cells should also be considered in future studies for a deeper understanding of the C/EBPβ–VCAM1 axis in KCs and increased opportunity for precise intervention.

In summary, MASLD increased C/EBPβ levels and activity in KCs, leading to significant alterations in the KC transcriptome and cellular functions and consequently exacerbated hepatic inflammation in MASLD. The underlying molecular mechanism involves increased transcriptional activation of C/EBPβ in the *Vcam1* promoter, contributing to KC-mediated increased VCAM1–integrin interaction and consequent immune cell infiltration. The discovery of the "C/EBPβ–VCAM1" axis in KCs provides a promising therapeutic target for tuning KC function in MASLD and deepens current understanding of liver inflammation in MASLD.

Affiliations

[1]*Department of Gastroenterology, Xin Hua Hospital Affiliated to Shanghai Jiao Tong University School of Medicine, Shanghai, China;* [2]*Department of Gastroenterology, Huadong Hospital, Fudan University, Shanghai, China;* [3]*State Key Laboratory of Reproductive Medicine, The Affiliated Taizhou People's Hospital of Nanjing Medical University, Taizhou School of Clinical Medicine, Nanjing Medical University, Nanjing, China;* [4]*Department of Gerontology, Huadong Hospital, Fudan University, Shanghai, China;* [5]*Shanghai Key Laboratory of Pediatric Gastroenterology and Nutrition, Shanghai, China*

Abbreviations

C/EBPβ, CCAAT/enhancer binding protein β; CRE, cis-regulatory element; DEG, differentially expressed gene; EmKC, embryonic KC; GO, gene ontology; HFHCD, high-fat and high-cholesterol diet; KC, Kupffer cell; LSEC, liver sinusoidal endothelial cell; MASH, metabolic dysfunction-associated steatohepatitis; MASL, metabolic dysfunction-associated steatotic liver; MASLD, metabolic dysfunction-associated steatotic liver disease; MoKC, monocyte-derived KC; MoMF, monocyte-derived macrophage; ND, normal diet; NPC, non-parenchymal cell;

RT-qPCR, reverse transcription quantitative PCR; TF, transcription factor; TSS, transcription start sites; VCAM1, vascular cell adhesion molecule 1.

Financial support

This work was supported by the Noncommunicable Chronic Disease-National Science and Technology Major Project of China (2023ZD0508700 to J-GF) and the National Natural Science Foundation of China (82270620 to Y-WC and 82170593 and 82470600 to J-GF).

Conflicts of interest

The authors have no conflicts to report.

Please refer to the accompanying ICMJE disclosure forms for further details.

Authors' contributions

Conceived and designed the project: J-GF, Y-WC. Performed the experiments: S-ZL, YX. Analyzed the data: S-ZL, YX, Y-SS. Contributed to the animal models: Y-QC, RX. Wrote the manuscript: S-ZL, YX, ML. Participated in discussing and revising the manuscript: all authors.

Data availability statement

CUT&Tag-seq and RNA-seq data were deposited in NCBI's Gene Expression Omnibus and are accessible through GEO Series accession numbers GSE273162 and GSE273163, respectively. All other data supporting the findings of this study are available from the corresponding authors upon reasonable request.

Acknowledgements

We thank Dr Hong-Wei Wang for assistance with manuscript preparation. We also thank Mr Chen-Zhi Guo and the Core Facility of Basic Medical Sciences, Shanghai Jiao Tong University School of Medicine, for their technological support in flow cytometry.

Supplementary data

Supplementary data to this article can be found online at https://doi.org/10.1016/j.jhepr.2025.101418.

References

Author names in bold designate shared co-first authorship

[1] Rinella ME, Lazarus JV, Ratziu V, et al. A multisociety Delphi consensus statement on new fatty liver disease nomenclature. J Hepatol 2023;79:1542–1556.

[2] **Targher G**, **Byrne CD**, **Tilg H**. MASLD: a systemic metabolic disorder with cardiovascular and malignant complications. Gut 2024;73:691–702.

[3] Schuster S, Cabrera D, Arrese M, et al. Triggering and resolution of inflammation in NASH. Nat Rev Gastroenterol Hepatol 2018;15:349–364.

[4] Mladenić K, Lenartić M, Marinović S, et al. The "Domino effect" in MASLD: the inflammatory cascade of steatohepatitis. Eur J Immunol 2024;54:e2149641.

[5] Simon TG, Roelstraete B, Khalili H, et al. Mortality in biopsy-confirmed nonalcoholic fatty liver disease: results from a nationwide cohort. Gut 2021;70:1375–1382.

[6] Heymann F, Tacke F. Immunology in the liver—from homeostasis to disease. Nat Rev Gastroenterol Hepatol 2016;13:88–110.

[7] Krenkel O, Tacke F. Liver macrophages in tissue homeostasis and disease. Nat Rev Immunol 2017;17:306–321.

[8] Guilliams M, Scott CL. Liver macrophages in health and disease. Immunity 2022;55:1515–1529.

[9] Ginhoux F, Guilliams M. Tissue-resident macrophage ontogeny and homeostasis. Immunity 2016;44:439–449.

[10] **Tran S**, **Baba I**, Poupel L, et al. Impaired Kupffer cell self-renewal alters the liver response to lipid overload during non-alcoholic steatohepatitis. Immunity 2020;53:627–640 e625.

[11] **Xiong X**, **Kuang H**, **Ansari S**, et al. Landscape of intercellular crosstalk in healthy and NASH liver revealed by single-cell secretome gene analysis. Mol Cell 2019;75:644–660 e645.

[12] Remmerie A, Martens L, Thone T, et al. Osteopontin expression identifies a subset of recruited macrophages distinct from Kupffer cells in the fatty liver. Immunity 2020;53:641–657 e614.

[13] **Chen S**, **Yang J**, Wei Y, et al. Epigenetic regulation of macrophages: from homeostasis maintenance to host defense. Cell Mol Immunol 2020;17:36–49.

[14] **Sakai M**, **Troutman TD**, **Seidman JS**, et al. Liver-derived signals sequentially reprogram myeloid enhancers to initiate and maintain Kupffer cell identity. Immunity 2019;51:655–670 e658.

[15] **Seidman JS**, **Troutman TD**, **Sakai M**, et al. Niche-specific reprogramming of epigenetic landscapes drives myeloid cell diversity in nonalcoholic steatohepatitis. Immunity 2020;52:1057–1074 e1057.

[16] **Li BH**, **He FP**, Yang X, et al. Steatosis induced CCL5 contributes to early-stage liver fibrosis in nonalcoholic fatty liver disease progress. Transl Res 2017;180:103–117 e104.

[17] van der Krieken SE, Popeijus HE, Mensink RP, et al. CCAAT/enhancer binding protein beta in relation to ER stress, inflammation, and metabolic disturbances. Biomed Res Int 2015;2015:324815.

[18] Huber R, Pietsch D, Panterodt T, et al. Regulation of C/EBP beta and resulting functions in cells of the monocytic lineage. Cell. Signal 2012;24:1287–1296.

[19] **Ren Q**, **Liu Z**, **Wu L**, et al. C/EBPβ: the structure, regulation, and its roles in inflammation-related diseases. Biomed Pharmacother 2023;169:115938.

[20] **Liu XL**, **Pan Q**, Cao HX, et al. Lipotoxic hepatocyte-derived exosomal microRNA 192-5p activates macrophages through Rictor/Akt/forkhead box transcription factor O1 signaling in nonalcoholic fatty liver disease. Hepatology 2020;72:454–469.

[21] **Guilliams M**, **Bonnardel J**, **Haest B**, et al. Spatial proteogenomics reveals distinct and evolutionarily conserved hepatic macrophage niches. Cell 2022;185:379. 6.e338.

[22] Kong DH, Kim YK, Kim MR, et al. Emerging roles of vascular cell adhesion molecule-1 (VCAM-1) in immunological disorders and cancer. Int J Mol Sci 2018;19:16.

[23] Kazankov K, Jorgensen SMD, Thomsen KL, et al. The role of macrophages in nonalcoholic fatty liver disease and nonalcoholic steatohepatitis. Nat Rev Gastroenterol Hepatol 2019;16:145–159.

[24] Barreby E, Chen P, Aouadi M. Macrophage functional diversity in NAFLD—more than inflammation. Nat Rev Endocrinol 2022;18:461–472.

[25] Daemen S, Gainullina A, Kalugotla G, et al. Dynamic shifts in the composition of resident and recruited macrophages influence tissue remodeling in NASH. Cell Rep 2021;34:108626.

[26] **Krenkel O**, **Puengel T**, Govaere O, et al. Therapeutic inhibition of inflammatory monocyte recruitment reduces steatohepatitis and liver fibrosis. Hepatology 2018;67:1270–1283.

[27] Guillot A, Winkler M, Silva Afonso M, et al. Mapping the hepatic immune landscape identifies monocytic macrophages as key drivers of steatohepatitis and cholangiopathy progression. Hepatology 2023;78:150–166.

[28] **Hendrikx T**, **Porsch F**, Kiss MG, et al. Soluble TREM2 levels reflect the recruitment and expansion of TREM2$^+$ macrophages that localize to fibrotic areas and limit NASH. J Hepatol 2022;77:1373–1385.

[29] Shi HX, Wang XB, Li F, et al. CD47-SIRPα axis blockade in NASH promotes necroptotic hepatocyte clearance by liver macrophages and decreases hepatic fibrosis. Sci Translational Med 2022;14.

[30] Barreby E, Strunz B, Nock S, et al. Human resident liver myeloid cells protect against metabolic stress in obesity. Nat Metab 2023;5:1188–1203.

[31] Kanamori Y, Tanaka M, Itoh M, et al. Iron-rich Kupffer cells exhibit phenotypic changes during the development of liver fibrosis in NASH. iScience 2021;24:102032.

[32] **Govaere O**, **Petersen SK**, **Martinez-Lopez N**, et al. Macrophage scavenger receptor 1 mediates lipid-induced inflammation in non-alcoholic fatty liver disease. J Hepatol 2022;76:1001–1012.

[33] Rahman SM, Schroeder-Gloeckler JM, Janssen RC, et al. CCAAT/enhancing binding protein beta deletion in mice attenuates inflammation, endoplasmic reticulum stress, and lipid accumulation in diet-induced nonalcoholic steatohepatitis. Hepatology 2007;45:1108–1117.

[34] **Schroeder-Gloeckler JM**, **Rahman SM**, Janssen RC, et al. CCAAT/enhancer-binding protein beta deletion reduces adiposity, hepatic steatosis, and diabetes in Lepr(db/db) mice. J Biol Chem 2007;282:15717–15729.

[35] Rahman SM, Janssen RC, Choudhury M, et al. CCAAT/enhancer-binding protein β (C/EBPβ) expression regulates dietary-induced inflammation in macrophages and adipose tissue in mice. J Biol Chem 2012;287:34349–34360.

[36] Rahman SM, Baquero KC, Choudhury M, et al. C/EBP beta in bone marrow is essential for diet induced inflammation, cholesterol balance, and atherosclerosis. Atherosclerosis 2016;250:172–179.

[37] **Ndoja A**, **Reja R**, Lee SH, et al. Ubiquitin ligase COP1 suppresses neuroinflammation by degrading c/EBPβ in microglia. Cell 2020;182:1156–1169 e1112.

[38] **Liao J**, **Chen G**, Liu X, et al. C/EBPβ/AEP signaling couples atherosclerosis to the pathogenesis of Alzheimer's disease. Mol Psychiatry 2022;27:3034–3046.

[39] Gehrke N, Schattenberg JM. Metabolic inflammation—a role for hepatic inflammatory pathways as drivers of comorbidities in nonalcoholic fatty liver disease? Gastroenterology 2020;158:1929–1947 e1926.
[40] Amit I, Winter DR, Jung S. The role of the local environment and epigenetics in shaping macrophage identity and their effect on tissue homeostasis. Nat Immunol 2016;17:18–25.
[41] T'Jonck W, Guilliams M, Bonnardel J. Niche signals and transcription factors involved in tissue-resident macrophage development. Cell Immunol 2018;330:43–53.
[42] Dorr D, Obermayer B, Weiner JM, et al. C/EBPβ regulates lipid metabolism and Pparg isoform 2 expression in alveolar macrophages. Sci Immunol 2022;7:eabj0140.
[43] **Troncoso MF**, **Díaz-Vesga MC**, Sanhueza-Olivares F, et al. Targeting VCAM-1: a therapeutic opportunity for vascular damage. Expert Opin Ther Targets 2023;27:207–223.
[44] Furuta K, Guo Q, Pavelko KD, et al. Lipid-induced endothelial vascular cell adhesion molecule 1 promotes nonalcoholic steatohepatitis pathogenesis. J Clin Invest 2021;131.
[45] **Rai RP**, **Liu Y**, Iyer SS, et al. Blocking integrin $\alpha_4\beta_7$-mediated CD4 T cell recruitment to the intestine and liver protects mice from western diet-induced non-alcoholic steatohepatitis. J Hepatol 2020;73:1013–1022.
[46] **Lavin Y**, **Winter D**, **Blecher-Gonen R**, et al. Tissue-resident macrophage enhancer landscapes are shaped by the local microenvironment. Cell 2014;159:1312–1326.
[47] Otsuka H, Yagi H, Endo Y, et al. Kupffer cells support extramedullary erythropoiesis induced by nitrogen-containing bisphosphonate in splenectomized mice. Cell Immunol 2011;271:197–204.
[48] Dutta P, Hoyer FF, Grigoryeva LS, et al. Macrophages retain hematopoietic stem cells in the spleen via VCAM-1. J Exp Med 2015;212:497–512.
[49] **Li D**, **Xue W**, **Li M**, et al. VCAM-1^+ macrophages guide the homing of HSPCs to a vascular niche. Nature 2018;564:119–124.

Keywords: MASLD; MASH; Kupffer cell; VCAM1; C/EBPβ.
Received 17 September 2024; received in revised form 26 March 2025; accepted 31 March 2025; Available online 15 April 2025